Attitude control of apricot during orientation transmission

Ding Xiangyan, Wang Chunyao*, Huang Chunyang, Luo Jianqing

(*School of Mechanical Engineering, Xinjiang University, Urumqi 830047, China*)

Abstract: The kinetic characteristics of apricots during orientation transmission were studied to provide a basis for improving the structure of the transmission device. Previous studies have generally focused on the development of orientation devices, but few studies have been conducted to analyze the mechanisms of orientation. In order to study the attitude control in the orientation mechanisms, an orthogonal combination test was performed and a rigid kinetic model for a monosymmetric apricot was developed based on Euler's kinetic equations with the modified Rodrigue parameters (MRPs). Kinetic simulation and analysis based upon the attitude control law were conducted and an attitude control simulation platform was created. The simulation results showed that the orientation transmission system for monosymmetric apricots was globally convergent and tended to stable. The experimental torques also affected the orientation success rates. The calculated average experimental torque value (0.164 N·m) was consistent with the maximum control torque value (0.16478 N·m) when the system was in a stable state in Simulink. The consistency between the simulation result and the calculated control torque validates the correctness of the designed control torques.

1 Introduction

Monosymmetric fruit transmitted by mechanical platforms are normally oriented automatically with the help of machines that take advantage of their inherent physical properties. Previous studies generally focused on the development of orientation devices, few studies have been conducted to improve the mechanisms of orientation. In the research focused on the application of machine vision systems to apple surface inspection

conducted by Rehkugler and Throop[1-3] in 1986, a method of apple orientation was developed in order to ensure accurate inspection by preventing the fruit stems and calyxes from being identified as damage. In 2008, Narayanan and Lefcour[4-6] introduced the use of an industrial camera to monitor the pure rolling of apple along an incline. They found that the random motion of apples gradually turned into automatic orientation.

In light of the widespread use of stability theory in agricultural machinery, rigid body dynamic was used to investigate the orientation mechanism of monosymmetric fruit during transmission. The results of the experiment indicated that during actual operation, the periodic motion of the coupled system composed of a flexible holding piece (leaf spring) and a rigid apricot modified the orientation of apricot by creating a force between the two parts, which was similar to an exciting force[7-8]. As a complex nonlinear motion, the delivery of the apricot could be greatly affected by any mechanical part which could cause chaos phenomeno n in a system[9-11]. In this study, the phase planes of apricots were presented using

quaternions. The control torque equations were obtained through calculation[12-16] and the torque control charts were obtained by Simulink simulation. The unique state of motion of a monosymmetric apricot during orientation transmission was displayed by phase portraits in order to analyze the stability of the system.

2   Materials and methods

2.1   Experiment design and equipment

The experiment was carried out using a KMT dynamic strain measurement system (7V22, SICK, Germany). Figure 1 shows the wire layout and data acquisition device of the KMT system.
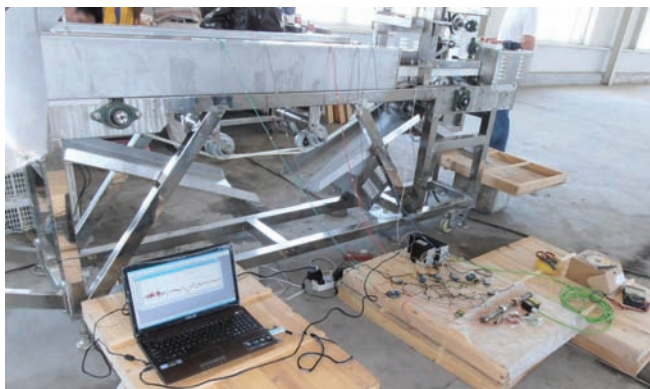
Figure 1   The KMT system

The resistance strain gauge was first pasted onto the test sample to allow it to extend and compress with the sample. Because of the linear relationship between mechanical strain and change in resistance over the time range in which Hooker's law is valid, the mechanical strain can be inferred from the measurements of resistance. To determine the relationship between external load and strain, the load and corresponding strain were measured and plotted on a graph after static calibration of the leaf springs was performed. Subsequently, a curve was fitted to the data points, as shown in Figure 2. The resultant linear fitted function was $y=0.0785x+0.3373$. Then loads can be calculated from their corresponding strain values using this function.

A $L_9(3^4)$ orthogonal array testing was performed. According to the test requirement, width of entrance channel, clamping belt speed and apricots diameter size were chosen as the experimental factors. Factors and levels of the orthogonal test are shown in Table 1 and

more details about how to perform the experimental can be found in reference[17].
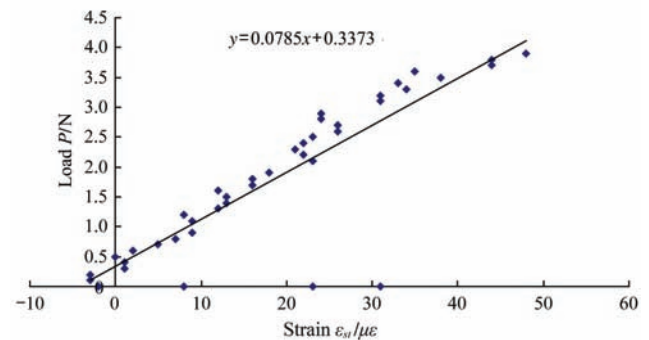
Figure 2   Linear relationship between the external load and the strain

Table 1   Factors and levels of orthogonal test

Level	Width of entrance channel/m	Clamping belt speed /m·s^{-1}	Apricots diameter size /m
1	0.17	0.22	0.34-0.35
2	0.25	0.28	0.35-0.36
3	0.33	0.42	0.36-0.37

After the orientation was carried out, the final states of the apricots were recorded by a high-speed camera, and the strain values were collected by the KMT system.

As shown in Figure 3, the resistance strain gauges are pasted onto the holding pieces to get the strain values. The holding belts are driven by the driven shaft and driving shaft. The holding belts hold the apricot and the holding piece is closed, while the transmission belt moves forward with the apricots. They help the apricot transform from the initial random state into final state. During the whole process, the transmission belt and the holding belt can be treated as flexible bodies.
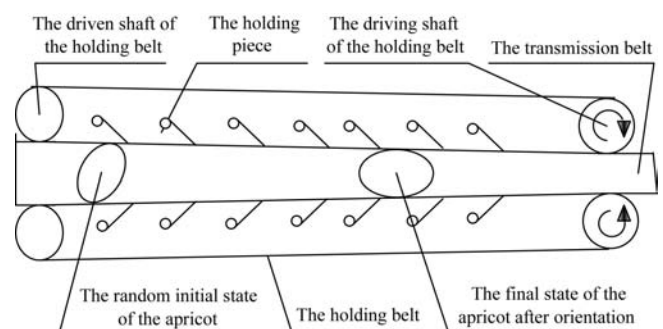
Figure 3   Apricot state in orientation device

2.3   Kinematic model of monosymmetric fruit

The widely-used methods for the description of the attitude include quaternions, Euler angles, and Rodrigue parameters[18-22], which are generally interconvertible. The quaternion method requires only three parameters,

method of Euler angles exhibits singularities, and the modified Rodrigue parameterization (MRPs) exhibits no singularity and requires only three independent variables. In this research, the attitude of the apricot is described using MRPs, and expressed as $\sigma=[\sigma_1\ \sigma_2\ \sigma_3]^T$. The relationships between the elements of MRPs and quaternions can be given as:

$$\sigma_1 = \frac{q_1}{1+q_0}, \ \sigma_2 = \frac{q_2}{1+q_0}, \ \sigma_3 = \frac{q_3}{1+q_0} \quad (1)$$

Therefore, the MRPs-based kinematics equations for apricot can be obtained:

$$\dot{\sigma} = \frac{1}{4}\begin{bmatrix} 1-\sigma^2+2\sigma_1^2 & 2(\sigma_1\sigma_2-\sigma_3) & 2(\sigma_1\sigma_3+\sigma_2) \\ 2(\sigma_2\sigma_1+\sigma_3) & 1-\sigma^2+2\sigma_2^2 & 2(\sigma_2\sigma_3-\sigma_1) \\ 2(\sigma_3\sigma_1-\sigma_2) & 2(\sigma_3\sigma_2+\sigma_1) & 1-\sigma^2+2\sigma_3^2 \end{bmatrix}\begin{bmatrix} \omega_1 \\ \omega_2 \\ \omega_3 \end{bmatrix}$$
$$(2)$$

where, $\sigma^2=\sigma_1^2+\sigma_2^2+\sigma_3^2$, and ω_1, ω_2 and ω_3 are the components of the apricot's angular velocity in the body-fixed frame, relative to the inertial reference frame.

Rearrange Equation (2) as:

$$\dot{\sigma} = \frac{1}{4}[(1-\sigma^T\sigma)I_{3\times3}+2\tilde{\sigma}+2\sigma\sigma^T]\omega = \frac{1}{4}[A(\sigma)]\omega \quad (3)$$

where,

$$A(\sigma) = (1-\sigma^T\sigma)I_{3\times3}+2\tilde{\sigma}+2\sigma\sigma^T \quad (4)$$

$$\tilde{\sigma} = \begin{bmatrix} 0 & -\sigma_3 & \sigma_2 \\ \sigma_3 & 0 & -\sigma_1 \\ -\sigma_2 & \sigma_1 & 0 \end{bmatrix} \quad (5)$$

2.4 Kinetic model of monosymmetric fruit

The forces acting on the apricot on the orientation device were determined by analyzing the apricot's actual state of motion during transmission, as shown in Figure 4.
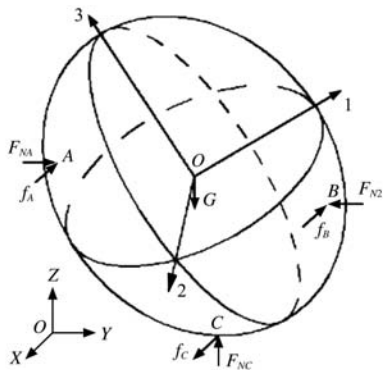
Figure 4　Fruit position at any time

During transmission, the apricot was under the effect of three major forces: the holding force F, friction f, and

gravity G. M denotes the resultant moment. The moment about the X, Y, and Z axes of the body-fixed frame is represented by M_x, M_y, and M_z, respectively.

A three-dimensional rectangular coordinate system ($O_{1,2,3}$) was created with its origin fixed at the apricot's center of mass and axes parallel to the apricot's principal axes of inertia. The external principal moment M was decomposed into three components about the principal axes of inertia. Then, Euler's kinetic equations were used as the differential equations to describe the planar motion of the overall apricot transmission system. The Euler's kinetic equations for monosymmetric fruit are as follows:

$$\begin{cases} I_1\dot{\omega}_1+(I_3-I_2)\omega_2\omega_3 = T_{c1}+T_{g1} \\ I_2\dot{\omega}_2+(I_1-I_3)\omega_3\omega_1 = T_{c2}+T_{g2} \\ I_3\dot{\omega}_3+(I_2-I_1)\omega_1\omega_2 = T_{c3}+T_{g3} \end{cases} \quad (6)$$

where, T_{c1}, T_{c2}, and T_{c3} represent control torques; T_{g1}, T_{g2}, and T_{g3} are disturbance torques; I_1, I_2, and I_3 denote the moments of inertia about the three principal axes of inertia. The equations above can be rearranged as follows:

$$\dot{\omega} = \begin{bmatrix} \dot{\omega}_1 \\ \dot{\omega}_2 \\ \dot{\omega}_3 \end{bmatrix} = \begin{bmatrix} \dfrac{(I_2-I_3)}{I_1}\omega_2\omega_3 \\ \dfrac{(I_1-I_3)}{I_2}\omega_1\omega_3 \\ \dfrac{(I_1-I_2)}{I_3}\omega_2\omega_1 \end{bmatrix} + \begin{bmatrix} \dfrac{T_{c1}}{I_1} \\ \dfrac{T_{c2}}{I_2} \\ \dfrac{T_{c3}}{I_3} \end{bmatrix} + \begin{bmatrix} \dfrac{T_{g1}}{I_1} \\ \dfrac{T_{g2}}{I_2} \\ \dfrac{T_{g3}}{I_3} \end{bmatrix} \quad (7)$$

When virtual control torque U_c and virtual disturbance torque U_g are applied, the Euler's kinetic equation for monosymmetric fruit can be expressed as:

$$\dot{\omega} = U_c+U_g \quad (8)$$

2.5 Design of attitude control system for monosymmetric fruit

Combining Equations (3) and (8), yields:

$$\ddot{\sigma} = \frac{1}{4}[\dot{A}(\sigma)\omega+A(\sigma)\dot{\omega}] = \frac{1}{4}[\dot{A}(\sigma)\omega+A(\sigma)U_c+A(\sigma)U_g]$$
$$(9)$$

assuming that:

$$\frac{1}{4}[\dot{A}(\sigma)\omega+A(\sigma)U_c] = -K_1\sigma-K_2\dot{\sigma} \quad (10)$$

where, K_1 and K_2 represent the diagonal matrices consisting of the proportionality coefficients k_1 and the differential coefficients k_2 of the feedback control law,

respectively.

Substituting Equation (10) into Equation (9) yields the equation describing the closed-loop control system:

$$\ddot{\sigma} + K_2\dot{\sigma} + K_1\sigma = \frac{1}{4}A(\sigma)U_g \qquad (11)$$

According to the design principle of second-order systems in classical control theory, k_1 and k_2 can be chosen as controller parameters. In the presence of an attitude tracking command σ_0, the control law can be expressed as $k_1(\sigma_0 - \sigma) - k_2\dot{\sigma}$. Substituting the expression into Equation (10), gets:

$$\frac{1}{4}[\dot{A}(\sigma)\omega + A(\sigma)U_c] = K_1(\sigma_0 - \sigma) - K_2\dot{\sigma} \qquad (12)$$

Therefore, the virtual control input U_c is given by:

$$U_c = -A(\sigma)^{-1}[4K_1(\sigma_0 - \sigma) - K_2\dot{\sigma} + \dot{A}(\sigma)\omega] \qquad (13)$$

Where,

$$\dot{A}(\sigma) = -(\dot{\sigma}^T\sigma + \sigma^T\dot{\sigma})I_{3\times3} + 2\dot{\tilde{\sigma}} + 2\dot{\sigma}^T\sigma + 2\sigma^T\dot{\sigma} \qquad (14)$$

Based on the calculated virtual control input $U_c=[U_{c1} \ U_{c2} \ U_{c3}]^T$, the actual torque needed for attitude control can be calculated by Equation (8):

$$\begin{bmatrix} T_{c1} \\ T_{c2} \\ T_{c3} \end{bmatrix} = \begin{bmatrix} I_1U_{c1} \\ I_2U_{c2} \\ I_3U_{c3} \end{bmatrix} - \begin{bmatrix} (I_2 - I_3)\omega_2\omega_3 \\ (I_3 - I_1)\omega_3\omega_1 \\ (I_1 - I_2)\omega_1\omega_2 \end{bmatrix} \qquad (15)$$

2.6   Simulation and analysis of apricot attitude control

The apricot was treated as an ellipsoid, which can be represented by the following equation:

$$\frac{x^2}{a^2} + \frac{y^2}{b^2} + \frac{z^2}{c^2} = 1 \qquad (16)$$

For the actual apricot shown in Figure 4, in which Equation (16) takes 1-axis, 2-axis, 3-axis as x-axis, y-axis, z-axis, respectively. Then, $2a$=0.38 m, $2b$=0.42 m, $2c$=0.44 m, and M=0.03 kg, where a and b are the equatorial radiuses along the x-axis and y-axis, respectively, and c is the polar radius along the z-axis.

The following equations were used to calculate the moments of inertia:

The moment of inertia about the x, y, z-axis:

$$\begin{bmatrix} J_1 \\ J_2 \\ J_3 \end{bmatrix} = \begin{bmatrix} I_x \\ I_y \\ I_z \end{bmatrix} - \begin{bmatrix} \iiint_\Omega (y^2 + z^2)\rho(x,y,z)dv \\ \iiint_\Omega (x^2 + z^2)\rho(x,y,z)dv \\ \iiint_\Omega (y^2 + x^2)\rho(x,y,z)dv \end{bmatrix} = \begin{bmatrix} 0.925 \\ 0.864 \\ 0.821 \end{bmatrix} kg\cdot m^2$$

$$(17)$$

Simulation was conducted to analyze the stability of monosymmetric fruit in the Simulink environment. First, a Simulink simulation framework with five modules was designed, including an absolute angular velocity calculation module, a quaternion integration module, an attitude angle calculation module, an attitude angular velocity calculation module, and a control module (Figure 5).
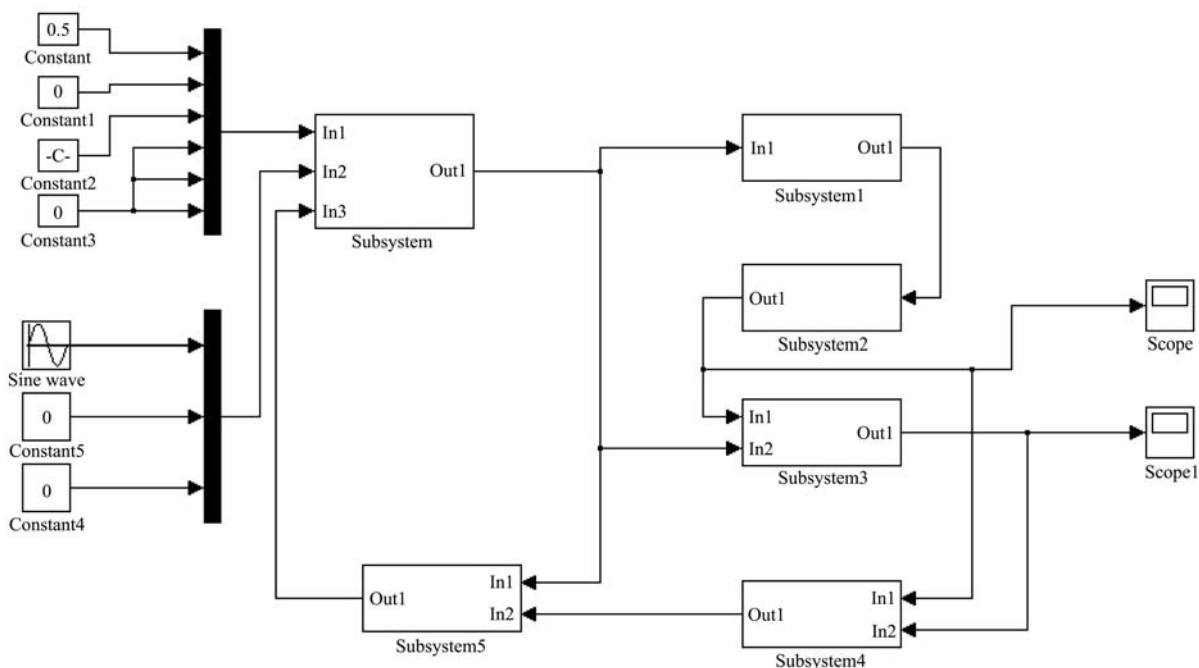
Figure 5   Simulink simulation framework

3   Results and discussion

The initial parameters of the apricot in the simulation (Figure 5) were mass of apricot m=0.03 g and width of entrance channe $2l$=2a.   The acceleration of gravity g is 9.8 m/s^2.   The initial quaternion value was $\left[\frac{1}{2} \quad 0 \quad \frac{\sqrt{3}}{2} \quad 0 \right]^T$, and the initial attitude angular velocity was $[0\ 0\ 0]^T$ rad/min.   The controller parameters were k_1=1 and k_2=2, the control torque limit was set at 0.1 N·m, and the moment of inertia matrix was $\begin{bmatrix} 0.925 & 0 & 0 \\ 0 & 0.864 & 0 \\ 0 & 0 & 0.821 \end{bmatrix}$ kg·m^2.

Based on these conditions, the integration step was set at 0.05 s and the control cycle was 0.1.   Figures 6a-6d show the results of simulation when the simulation time T_0 was adjusted to 500, 861, 1000, and 1080.   The top figure in each case shows the torque variation with the time, the middle figure shows the three-dimensional phase portrait of the angular velocity, and the bottom figure shows the Y-Z phase plane of the apricot.

Particularly revelatory is, if the unit is set as N·m, some details will not show in the figures, so the units in Figure 6 are N·mm.

As shown in Figure 6, the system in the case of (a) was stably convergent, and the torque peaked at 0.155 N·m.   In the case of (b), the system converged steadily, and the maximum torque peaked at 0.164 N·m after the system reached a stable state.   In the case of (c), as the simulation time increased, the system also tended to converge toward stability, and the torque showed big fluctuations and jumps.   In the case of (d), the torque varied in a stepwise manner.   These results indicated that attitude control law was applicable to the first three cases except the last.

Then, the orientation success rates and average strain values in the nine tests of the experiment were obtained by collating the collected data.   The load values were calculated using the function F=0.0785ε+0.3373.   The average values of strain when the actual load was F, the values of corresponding load, dynamic load and experimental torque were also calculated, as shown in Table 2.
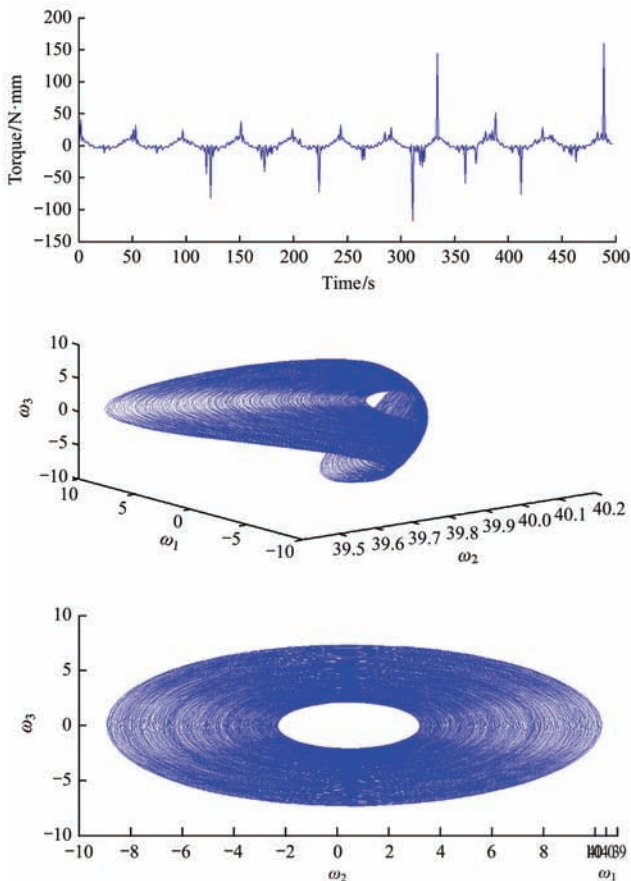
a. Simulation time of 500

b. Simulation time of 861

c. Simulation time of 1000   d. Simulation time of 1080
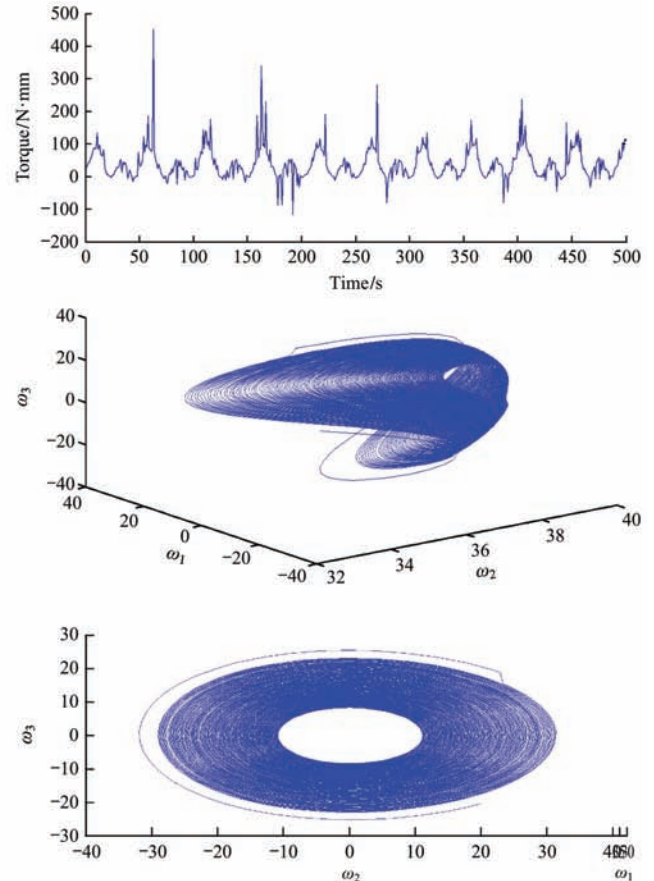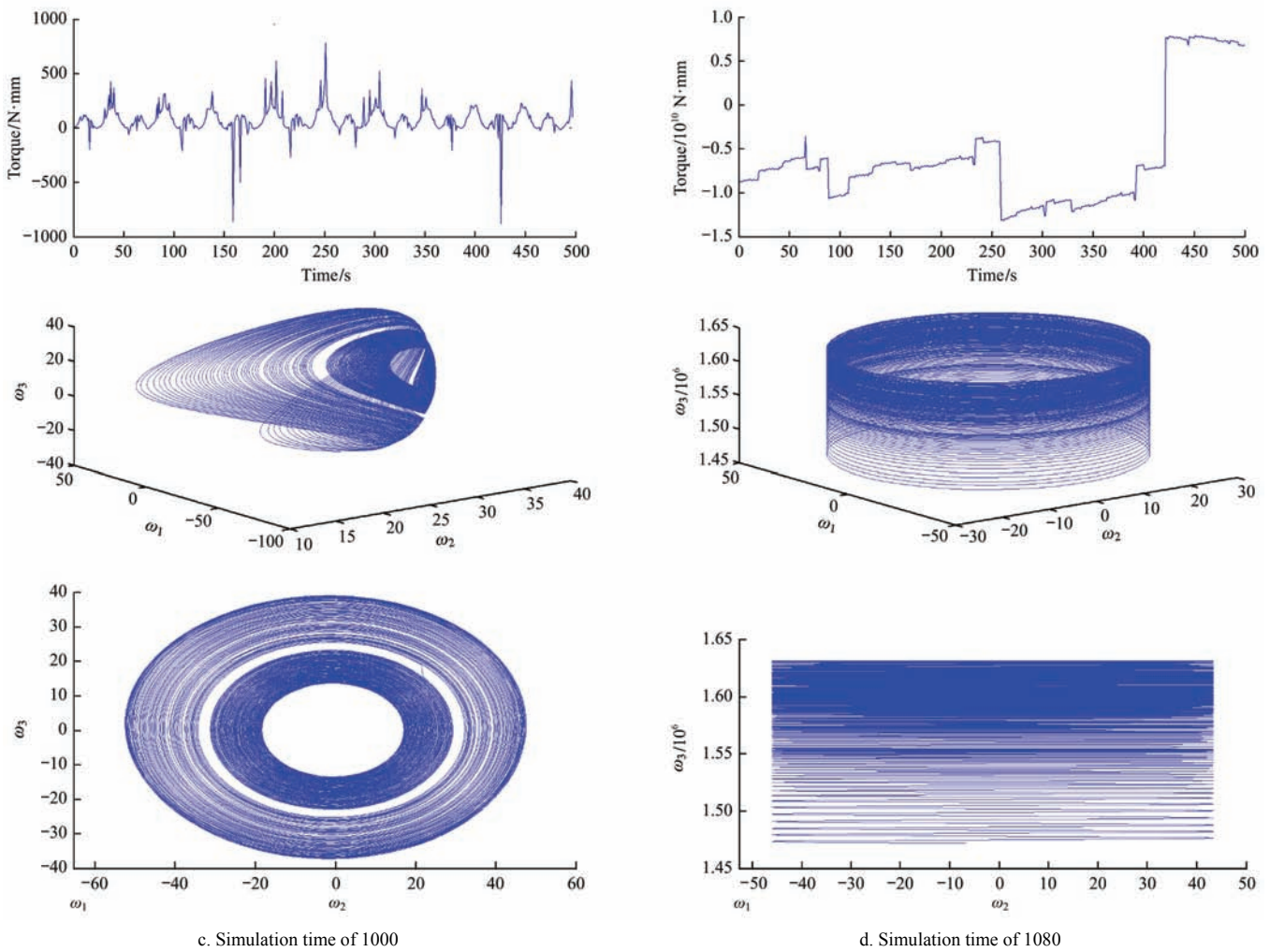
Figure 6   Simulink simulation results

Table 2   Table of experimental data

Test case	1	2	3	4	5	6	7	8	9
Orientation success rate/%	92.3	89.2	88.1	100	94.4	93.3	93.9	93.9	95.8
Strain $\varepsilon_{st}/\mu\varepsilon$	−400	−405	−421.5	−395.5	−396.5	−388	−367.5	−379	−369
Load P/N	−31.1	−31.4	−32.8	−30.7	−30.8	−30.1	−28.5	−29.4	−28.6
Dynamic load factor k_d	3.12	3.74	3.47	4.56	4.9	4.78	2.84	3.71	3.09
Dynamic load F_d /N	−48.5	−58.7	−56.8	−70	−75.4	−72	−40.5	−54.6	−44.2
Experimental torque U/N·m	−0.1276	−0.1725	−0.182	−0.1844	−0.2218	−0.2306	−0.1066	−0.1604	−0.1417

The three-dimensional phase portraits indicate that the apricots rotated around the shortest axis and tended to be stable in the first three cases, while they rotated around the longest axis and only gradually stabilized in the last case. The angular displacements of the apricots from the principal axes of inertia increased with increasing external torques. The motion of apricots within the nonlinear system can result in the system's self-oscillation. The system became more stable as its time evolution gradually weakened, which indicates that the system is globally convergent and becomes

progressively more stable. When the control torque was in the 0.155-0.164 N·m range, the system was in a stable state, and the apricots' angular velocities tend to be stable and free from jump.

Figure 7 shows a chart of the orientation success rates and experimental torques from Table 2. The figure shows that the orientation success rates were largely in the range of 92%-96%. Therefore, the points within this range were selected for the calculation of experimental torques. According to the results of the calculations, the average experimental torque was 0.16478 N·m. This

result is consistent with the maximum control torque (0.164 N·m) when the system was in a stable state in Simulink simulation, thus demonstrating the correctness of the control system in the orientation transmission of monosymmetric fruit.
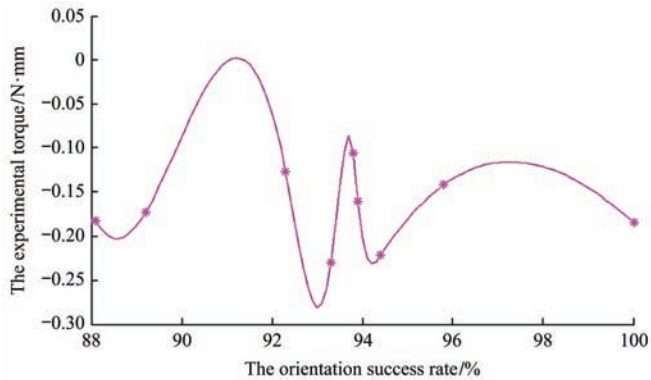
Figure 7   Orientation success rate–experimental torque

4   Conclusions

Analysis of the simulation results suggests that the system is globally convergent and becomes progressively more stable.   Moreover, when the control torque was in the 0.155-0.164 N·m range, the system was in a stable state, and the apricots' angular velocities tended to be stable and free from jump.   This range is therefore recommended for future systems.

In the orthogonal array testing, the final states of the oriented apricots were recorded by a high-speed camera, and the strain values of the holding pieces were collected by the KMT system.   The calculated average experimental torque was 0.16478 N·m, which was consistent with the maximum control torque (0.164 N·m) when the system was in a stable state in the Simulink simulation.

The simulation study of monosymmetric fruit's attitude during orientation transmission shows that when a small disturbance was applied to the stable system, the system gradually got back to a stable state after the variation.   A self-adaptive control system was designed for such systems.   The simulation demonstrated that this method was effective for the controlling, monitoring, and assessment of unknown variables.   The correctness of the control system was validated through an experiment. This research is expected to provide a basis for research on the orientation transmission of monosymmetric fruit.

[References]

[1]   Lefcourt A M, Narayanan P, Tasch U, Kim M S, Reese D, Rostamian R, et al.   Orienting apples for imaging using their inertial properties and random apple loading.   Biosystems Engineering, 2009; 104(1): 64–71.

[2]   Narayanan P, Lefcourt A M, Tasch U, Rostamian R, Abraham Grinblat, Kim M S.   Theoretical aspects of orienting fruit using stability properties during rotation. Portland Oregon: ASABE 2006. Paper No.061144. St. Joseph, Mich., ASABE

[3]   Narayanan P, Lefcourt A M, Tasch U, Rostamian R, Kim M S.   Tests of the ability to orient apples using their inertial properties.   2007. ASABE Paper No.076246. St. Joseph, Mich., ASABE.

[4]   Lefcourt A M, Kim M S, Chen Y R.   Detection of fecal contamination on apples with nanosecond-scale time-resolved imaging of laser-induced fluorescence. Applied Optics, 2005; 44(7): 1160–1170.

[5]   Lefcourt A M, Narayanan P, Tasch U, Rostamian R, Kim M S, Chen Y R.   Algorithms for parameterization of dynamics of inertia-based apple orientation.   Applied Engineering in Agriculture, 2008; 24(1): 123–129.

[6]   Zheng A Q, Cao Y, Zhao Y.   Practical textbook of MATLAB.   Beijing: Publishing House of Electronics Industry, 2004; 5.

[7]   Huang C Y, Wang C Y.   Application and research apricots of directional transport process using quaternion.   Journal of Agricultural Mechanization Research, 2015; 37(4): 32–34.

[8]   Liu Y Z, Hong J Z, Yang H X.   Multirigid-body-system dynamics.   Beijing: Higher Education Press, 1989: pp. 30-64.

[9]   Luo L J, Li Y-S, Li T, Dong Q T.   Research and simulation of Lyapunovps exponents.   Computer Simulation, 2009; 22(12): 285–288.

[10]   Zhang Y H, Yuan W F.   Structure and application on Lyapunov function.   Journal of Yulin University, 2011; 21(6): 21–23.

[11]   Liu Y, Wu B, Cai X S.   Stability criteria of nonlinear impulsive differential equations with infinite delays.   Acta Mathematicae Applicatae Sinica, 2015; 31(4): 921–934.

[12] Luo J Q, Wang C Y.   Dynamic stability of apricots motion in their directional conveying.   Journal of Vibration and Shock, 2015; 34(13): 115–120.

[13] Yang B, Zhou J, Guo J G.   Study on dynamics modeling of missile with deflectable nose.   Acta Aeronautica Et Astronautica Sinica, 2008; 29(4): 909–913.

[14] Chapman S J.   MATLAB Programming.   Beijing: Science Press, 2007; pp. 30–73.

[15] Ding H.   Realization of phase plane for higher order nonlinear control system based on simulink.   Journal of Electrical & Electronic Education, 2013; 35(3): 15.

[16] Ismail Z, Varatharajoo R, Ajir R, Rafie A S M.   Enhanced attitude control structure for small satellites with reaction wheels.   Aircraft Engineering and Aerospace Technology, 2015; 87(6): 546–550.

[17] Ding X Y, Wang C Y, Luo J Q.   KMT dynamic strain measurement system application in fruit orientation. Journal of Agricultural Mechanization Research, 2015; 37(6): 146–150.

[18] Huang T G, Wang L, Su J B.   Nonlinear disturbance rejection control of unmanned aerial vehicle attitude. Journal of Control Theory & Applications, 2015; 4: 456–463.

[19] Jia R C.   Attitude estimation base on gravity/magnetic assisted Euler angle UKF.   Journal of Optics and Precision Engineering, 2014; 22(12): 3280–3286.

[20] Mazinan A H.   High-precision full quaternion based finite-time cascade attitude control strategy considering a class of overactuated space systems.   Human-centric Computing and Information Sciences, 2015; 5(1): 1–14.

[21] Zhao X M, Yang L, Hui F, Shi X, Hao R R, Wang W X. Three-dimensional vehicle attitude estimation using modified invasive weed optimized particle filter.   International Journal of Automotive Technology, 2014; 15(7): 1143–1154.

[22] Yonmook P.   Robust and optimal attitude control of spacecraft with disturbances.   International Journal of Systems Science, 2015; 46(7): 1222–1233.